



## Estimation of the Petrophysical Model via Joint Inversion of Seismic and EM datasets

**Fabio Miotti**  
Schlumberger  
via Celeste  
Clericetti 42/A  
20133 Milano  
Italy  
fmiotti@slb.com

**Ivan Guerra**  
Schlumberger  
via Celeste  
Clericetti 42/A  
20133 Milano  
Italy  
IGuerra2@slb.com

**Federico Ceci**  
Schlumberger  
via Celeste  
Clericetti 42/A  
20133 Milano  
Italy  
FCeci@slb.com

**Andrea Lovatini**  
Schlumberger  
via Celeste  
Clericetti 42/A  
20133 Milano  
Italy  
ALovatini@slb.com

**Mehdi Paydayesh**  
Schlumberger  
Buckingham Gate,  
Gatwick,  
RH6 0NZ,  
United Kingdom  
MPaydayesh@slb.com

**Margaret Leathard**  
Schlumberger  
Buckingham Gate,  
Gatwick,  
RH6 0NZ,  
United Kingdom  
leathard1@slb.com

**Garrett Kramer**  
Schlumberger  
Level 5, 256 St.  
Georges Terrace,  
Perth, WA 6000,  
Australia  
gkramer@slb.com

### SUMMARY

Reservoir characterization objectives are to estimate the petrophysical properties of the prospective hydrocarbon traps and to reduce the uncertainty of the interpretation. In this framework, we present a workflow for petrophysical joint inversion of seismic and EM attributes to estimate the petrophysical model in terms of porosity and water saturation. This study realizes the joint inversion within the probabilistic structure provided by the Bayesian theory. The algorithm is applied to a real hydrocarbon exploration scenario to evaluate its contribution to the interpretation phase. 3D volumes of estimated porosity and saturation, show how the joint inversion of acoustic impedance and electrical resistivity can provide a quantitative description of the reservoir properties and with it a measure of uncertainty, which is consistent with the petrophysical model and observations.

**Key words:** Joint inversion, CSEM modelling, Rock modeling, Bayesian inversion

### INTRODUCTION

Estimating the oil and gas saturations can reduce costly drilling of un-productive reservoirs. Over the years, several studies showed the advantage of relating the geophysical attributes to rock properties to improve the prediction of the reservoir properties (Hilterman, 2001). In this framework several techniques are available; some are based on the deterministic approaches, while others involve the use of statistics to mitigate the simplifications introduced by rock physics models (Bachrach, 2006; Dell'Aversana et al., 2011).

Many examples using only seismic inversion attributes such as acoustic impedance (AI), Vp/Vs ratio, Poisson's ratio and density, have been discussed in the literature (Barclay et al 2008). Other authors studied the integration of seismic attributes (e.g., acoustic impedance, Vp/Vs) with EM attribute, mainly the resistivity model, which is obtained by **controlled-source** electromagnetic (CSEM) inversion, (Gao et al., 2012; Chen and Dickens, 2009; Chen et al., 2007; Giraud et al., 2013). The benefits of

using electrical resistivity attribute within an interpretation workflow was shown by different studies (De Stefano et al., 2011; Miotti et al., 2010), which emphasizes the importance of integrating different geophysical attributes to improve interpretation.

To achieve this objective we developed a novel technique to estimate the petrophysical model in terms of porosity and water saturation. The proposed method performs the petrophysical joint inversion (PJI), pixel based, of acoustic impedance and electrical resistivity models, through formal Bayesian estimation, assuming Gaussian probability density function for model parameters and input data. In this framework, rock physics models are involved as forward models to form a proper link between data input (AI and resistivity) and the petrophysical parameters, porosity and water saturation, (Carcione et al., 2007; Schön, 1996).

### METHOD AND RESULTS

#### Constitutive equations

According to the rock cross property concept introduced by Carcione, (Carcione et al., 2007; Dell'Aversana et al., 2011), for integrating heterogeneous measurements, we must define some constitutive equations that link rock properties with well-log measurements, Figure 1. In this example we are assuming isotropic media.

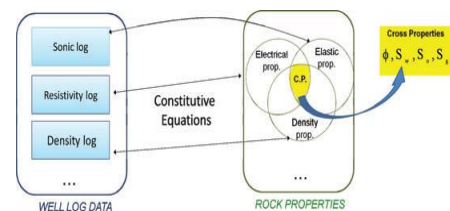


Figure 1: Cross properties, conceptual scheme.

Many rock physics models are available and their efficacy depends on the particular lithology of the sediments (Schön 1996). To predict the compressional velocity in homogeneous, isotropic, elastic media we consider the relation:

$$V_p = \sqrt{\frac{K_G + \frac{4}{3}\mu}{\rho}}$$

where  $\mu$  is the effective shear modulus of the porous rock. To predict this value we use the Krief model (A is an empirical parameter, 3 is the most common value):

$$\mu = \mu_s \cdot (1-\phi)^{\frac{A}{1-\phi}}$$

$\mu_s$  is the shear modulus of the mineral making up the rock and  $\phi$  represents the rock porosity.

The term  $\rho$  represents the composite density of the bulk that is defined by the following volumetric average (three-phase fluid):

$$\rho = (1-\phi) \cdot \rho_s + \phi \cdot (S_w \rho_w + S_o \rho_o + S_g \rho_g)$$

In the previous formula the suffix 'w' indicates water, 'o' is oil, 'g' is gas, and 's' represents the solid phase. The term  $K_G$  is the effective bulk modulus of the saturated rock, defined by the Gassmann model:

$$K_G = \frac{K_s - K_m + \phi \cdot K_m \cdot \frac{K_s}{K_f} - 1}{1 - \phi - \frac{K_m}{K_s} + \phi \cdot \frac{K_s}{K_f}}$$

where:

- $K_s$  : bulk modulus of the mineral making up the rock
- $K_m$  : effective bulk modulus of the dry porous rock predicted, in this workflow, by the Krief model (A=3 is the most common value):

$$K_m = K_s \cdot (1-\phi)^{\frac{A}{1-\phi}}$$

- $K_{fl}$  : effective bulk modulus of the fluid phase predicted, in this workflow, by Wood's formula (three-phase fluid):

$$K_f = \left( \frac{S_w}{K_w} + \frac{S_g}{K_g} + \frac{S_o}{K_o} \right)^{-1}$$

To address the electrical resistivity the well known Archie model, (second formulation), is involved:

$$R = R_w \cdot S_w^{-n} \cdot \phi^{-m}$$

where

- R: effective resistivity of the saturated rock
- $R_w$ : water resistivity.
- $S_w$  : water saturation.
- m: cementation exponent.
- n: saturation exponent.

Previous rock models represent the constitutive equations that are able to constrain the inverse problem by providing a

petrophysical model that conforms to the physics of the phenomenon.

### Input data

As input data we consider:

- The seismic attributes such as acoustic impedance, density and Poisson's ratio models.
- The resistivity model resulting from the CSEM inversion.

All models are defined within the same grid in order to have the same number of cells (Figure 2). Because the CSEM inversion produces a low-resolution model with respect to the seismic model, we mitigate this limitation exploiting the transverse resistance principle, (Constable 2010, Metha et al 2005). The approach is the following; first, we need to derive the resistive anomaly within the model resulting from the CSEM inversion as:  $R_{anomaly} = R_{CSEM} - R_{back}$ . Where  $R_{back}$  is a background resistivity model, which is generally defined based on well logs and/or geological information. In the second step, by applying the transverse resistive principle to the  $R_{anomaly}$ , we bound the resistive anomaly within the geological boundaries that are supposed to contain hydrocarbon.

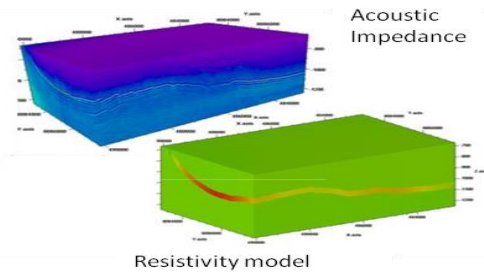


**Figure 2: Input data, acoustic impedance, and resistivity model after the transverse resistance processing.**

### MODELING AND INVERSION

For modeling, we follow Tarantola's approach on inverse problems, (Tarantola, 2005). We start from the non-linear relation linking model parameters to the input data:

$$d = g(m)$$

We distinguish the vector  $m$  that defines the unknown model parameters in the model space, (porosity and water saturation in the bi-phase configuration), while the  $d$  vector represents the input data, (acoustic impedance and electrical resistivity values). According to the Bayesian theory, the state of information on the model parameters is described by the prior model  $m_{prior}$  and by  $C_M$ , the covariance matrix that takes into account its uncertainties. The uncertainty associated with the observed data is captured by  $C_D$ , which is the data covariance matrix. We assume Gaussian probability distribution for both model parameters and data. The solution of the inverse problem is obtained through an iterative procedure that linearizes the forward model around the current model  $m_k$  and obtains a new model  $m_{k+1}$ . At every iteration, the Jacobian matrix  $G_k$ , which contains the derivatives of the forward model equation with respect to the current model parameters, is numerically updated. The closed-form solution is:

$$m_{k+1} = m_{prior} - \left[ G_k^T C_d^{-1} G_k + C_M^{-1} \right]^{-1} G_k^T C_d^{-1} \cdot \left[ (g(m_k) - d) - G_k (m_k - m_{prior}) \right]$$

The iterative algorithm stops when:

$$\|m_{i,k+1} - m_{i,k}\| < \epsilon \quad \forall i = 1, \dots, L.$$

Where  $L$  represents the number of cells forming the petrophysical model and  $\epsilon$  is the predefined value that specifies a stopping criterion. Finally, we compute the posterior covariance matrix of the model  $C_{M,post}$ , which describes the uncertainty of the solution as:

$$C_{M,post} = \left( G_k^T C_d^{-1} G_k + C_M^{-1} \right)^{-1}.$$

The sensitivity analysis and regularization of the inverse procedure are both detailed by Dell'Aversana et al., (2011). The entire workflow is depicted in Figure 3.

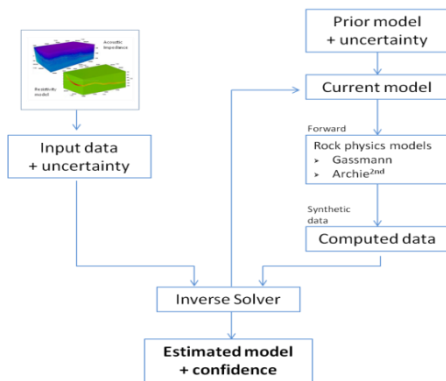


Figure 3: PJI inversion procedure.

**Example**

To evaluate its performances, the PJI technology was tested on a real exploration case. The input data consists of seismically derived acoustic impedance, Poisson’s ratio and density and CSEM derived electrical resistivity attributes.

The CSEM inversion provides the vertical and horizontal resistivity models, but since the PJI workflow assumes isotropic media, we chose as resistivity model, only the vertical component, because, for this survey, it is the most informative one. Seismic and CSEM inversions are carried out separately in their native domains, and consequently, different regularizations were applied to produce the acoustic impedance, Poisson’s ratio and density model in the seismic domain and the resistivity model in the electromagnetic domain.

The objective of the PJI is to describe quantitatively the petrophysical properties of a potential reservoir in terms of porosity and water saturation distribution within the 3D model. We apply the workflow within a selected area where both seismic attributes and resistivity models show anomalies as evidence of a potential reservoir. Guerra et al., (2013) explains how the joint interpretation for this survey was carried out, and we exploit their results to set up our analysis. The joint anomalies are depicted in Figure 4. Here we notice a low Poisson’s ratio and high resistivity values in the region of the seismic reflector.

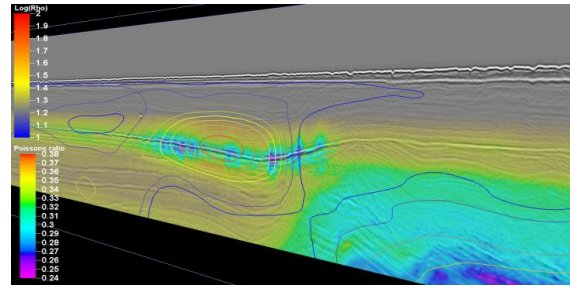


Figure 4: Seismic data co-rendered with Poisson’s ratio and vertical resistivity (contour lines). Both models show evidence that supports the presence of a potential gas reservoir. Image courtesy of Schlumberger.

Because well logs are not available in this area, we calibrated the prior rock model through the analysis of the scatter plots explaining the relations between the seismic attributes and the resistivity, (e.g., Poisson’s ratio versus resistivity), and between the seismic attributes themselves, (e.g., acoustic impedance versus Poisson’s ratio), (Hilterman, 2001). To test the contribution of the electrical resistivity in determining the petrophysical model, we carried out two different test involving as data input:

- Acoustic impedance and density model (Petrophysical Inversion - PI)
- Acoustic impedance and electrical resistivity model (Petrophysical Joint Inversion - PJI)

The Poisson’s ratio was not directly involved as data input because it is less sensitive to porosity respect to the acoustic impedance and density attributes. In contrast, his contribution was determinant to characterize the rock model in the previous calibration phase. We performed both tests and compared the results. The comparison is shown in Figure 6, which shows the porosity and water saturation models on the horizontal z-slice at a depth of -967 m, (Figure 5). The first row depicts the result of the petrophysical inversion while the second illustrates the result carried out from the petrophysical joint inversion. Both porosity estimates A and, D are consistent because this rock property is mainly derived by the AI attribute. In contrast, the comparison between the saturation estimates (B and C) exhibits the role of the resistivity attribute to discriminate fluids, (e.g., water from gas/oil). Specifically

- Model B is a “smooth” water saturation model because density and AI attributes are weakly sensitive to fluid substitution water-gas. For this reason the model shows several values close to the prior water saturation, here set to 0.5.
- The model C highlights the high sensitivity of resistivity with respect to resistive fluids such as oil and/or gas. The joint inversion strongly reduces the amount of water saturation corresponding to the resistive anomaly as evidence of a possible presence of gas saturation that is the preliminary assumption we are interested to support, (Guerra et al., 2013).

Since that the inverse algorithm performs a local optimization, it is important to define a representative prior model for the investigated area. Finally, we notice in the previous comparison the feature P, which shows high water saturation in the B model and the opposite trend in model C. We could deduce here a possible presence of oil, which under certain assumptions is a

resistive fluid with elastic properties similar to those of water. Because no well logs are available in this survey area, we assess the reliability of the results based on a cooperative interpretation based on scatter plot analysis. Having well logs in the survey it is possible to reduce the final uncertainty through both a more accurate calibration of the starting rock model and a more detailed assessment of the final results.

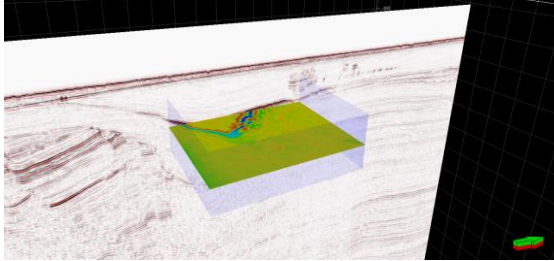


**Figure 5: Petrophysical joint inversion, mesh cube (transparent purple color) and porosity model on z-slice at -967m. Image courtesy of Schlumberger.**

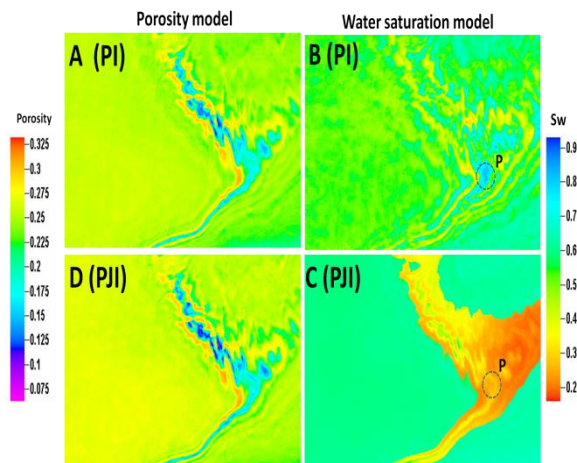


**Figure 6: Model comparison, petrophysical inversion vs PJI. A and B are the porosity and water saturation model resulting from the petrophysical inversion. D and C are the porosity and water saturation model resulting from the PJI. C model shows the contribution of EM attribute to discriminate the water content from resistive fluids (e.g., oil and/or gas).**

## CONCLUSIONS

The study presented in this paper shows the main feature of the algorithm we developed to get a robust estimation of the petrophysical model, starting from the seismic and resistivity attributes. The Bayesian theory is exploited to build the kernel of the inverse algorithm while the prior rock model is built based on realistic assumptions carried out after a scatter plot analysis. The results presented here evidence the contribution of the joint inversion of seismic and EM attributes to derive a quantitative description of the petrophysical model. Further, this study supports the role of the CSEM technology, which is an additional tool to be used in conjunction with seismic attributes to reduce uncertainty in prospect generation on West Loppa. Once prospects are identified, (with complimentary structural, stratigraphic and DHI's with CSEM resistivity indicators) the PJI is used as a quantifier for reservoir attributes. In order to improve this technology tests are in

place to exploit jointly all the information available from the seismic and resistivity attributes with the goal of being able to derive a more reliable petrophysical model. Finally, it is highly recommended to use well log data to better calibrate a representative rock model for the survey area, in order to improve the final result.

## ACKNOWLEDGMENTS

The authors thank WesternGeco and EMGS for allowing access to their multi-client datasets.

## REFERENCES

- Bachrach, R. 2006. Joint estimation of porosity and saturation using stochastic rock physics modeling, *Geophysics*, 71, O53-O63.
- Carcione J.M., Ursin B. and Nordskag J.I. 2007. Cross-property relations between electrical conductivity and the seismic velocity of rocks. *Geophysics* 72, 193–204.
- Chen J. and Dickens T.A. 2009. Effects of uncertainty in rock-physics models on reservoir parameter estimation using seismic amplitude variation with angle and controlled-source electromagnetics data. *Geophysical Prospecting* 57, 61–74.
- Constable S. 2010. Ten years of marine CSEM for hydrocarbon exploration. *Geophysics*, 75, No 5. PP75A67-75A81.
- Dell'Aversana P., Bernasconi G., Miotti F. and Rovetta D. 2011. Joint inversion of rock properties from sonic, resistivity and density well-log measurements. *Geophysical Prospecting* 59, 1144–1154.
- De Stefano M., Golfré Andreasi F., Re S., Virgilio M., Snyder F. F. 2011. Multiple-domain, simultaneous joint inversion of geophysical data with application to subsalt imaging, *Geophysics* 76 (3), p. R69-R80.
- Gao G., Abubakar A., Habashy T. M. 2012. Joint Inversion of electromagnetic and full-waveform seismic data, *Geophysics* 77 (3), p. wa3-wa18.
- Guerra I., Ceci F., Miotti F., Lovatini A., Milne G., Paydayesh M., Leathard M., Sharma A., Panzner M. and Gabrielsen P., 2013. Multi-measurement integration - a case study from the Barents Sea. *First Break*, 31, 55-61.
- Hilterman, F.J. 2001. *Seismic Amplitude Interpretation*. Distinguished Instructor Short Course, Distinguished Instructor Series, No. 4, SEG
- Miotti F., Bernasconi G., Rovetta D. and Dell'Aversana P. 2010. Estimation of rock properties from seismic, EM and gravity well-log measurements. *EGM 2010 International Workshop*.
- Schön J.H. 1996. *Physical Properties of Rocks: Fundamentals and Principles of Petrophysics*. Pergamon Press. ISBN 10008044346X.
- Tarantola A. 2005. *Inverse Problem Theory*. SIAM. ISBN9780898715729.